

Received:
14 March 2018
Revised:
4 May 2018
Accepted:
5 July 2018

Cite as: Ernest Gyan Bediako,
Emmanuel Nyankson,
David Dodoo-Arhin,
Benjamin Agyei-Tuffour,
Dariusz Łukowiec,
Błażej Tomiczek, Abu Yaya,
Johnson K. Efavi. Modified
halloysite nanoclay as a
vehicle for sustained drug
delivery.
Heliyon 4 (2018) e00689.
doi: [10.1016/j.heliyon.2018.e00689](https://doi.org/10.1016/j.heliyon.2018.e00689)



Modified halloysite nanoclay as a vehicle for sustained drug delivery

Ernest Gyan Bediako^{a,b}, Emmanuel Nyankson^{a,*}, David Dodoo-Arhin^a,
Benjamin Agyei-Tuffour^a, Dariusz Łukowiec^b, Błażej Tomiczek^b, Abu Yaya^a,
Johnson K. Efavi^a

^a Department of Materials Science and Engineering, University of Ghana, Legon, Accra, Ghana

^b Institute of Mechanical Engineering, Silesian University of Technology, Gliwice, Poland

* Corresponding author.

E-mail address: enyankson@ug.edu.gh (E. Nyankson).

Abstract

This paper presents the effect of modified halloysite nanotubes on the sustained drug release mechanisms of sodium salicylate. Acid treatment and composite polymer-halloysite modification techniques were adopted in this study. After each modification, sodium salicylate drug was loaded, and in vitro release properties were evaluated and compared with the raw unmodified halloysite nanotubes. The results obtained from SEM, TEM and FTIR analyses indicate that both acid treatment and composite formation have no effect on the tubular structure and morphology of halloysite. However, modification of the halloysite nanotubes did influence the drug release rate. In the acid treatment modification, there was an improved loading of sodium salicylate drug which resulted in the sustain release of large amount of the sodium salicylate. In the polymer/halloysite composite formation, a consistent layer of polymer was formed around the halloysite during the composite formation and thus delayed release providing sustained release of sodium salicylate drug over a longer period of time as compared to the acid treated and unmodified halloysite. The results from the invitro release were best fitted with the Higuchi and the Koresymer-Peppas models.

Keywords: Biomedical engineering, Materials science, Nanotechnology

1. Introduction

In recent years, sustained drug release systems that are manufactured from cheap, readily available and biocompatible materials have generated wider interests amongst researchers in the field of healthcare, pharmacy and material science. Conventionally, there are two ways by which drugs are delivered to tissues and organs in the body. These are by oral means and by injection. The purpose of drug delivery is to get an administered drug distributed to tissues or organs that are infected or diseased. The action of the drug on any other tissue or organ of the body that is not targeted mostly generates an unwanted side effect. In drug delivery, the level and duration of availability of drug cannot be sustained and controlled independently; only the size of the dosage and its frequency can be sustained and controlled. When a drug is administered, an initial high concentration of drug is made available to the tissues or organs through a phenomenon called “burst release”. The concentration decreases gradually as the drug is distributed [1, 2, 3]. In these modes of drug administration, the drug could degrade before reaching the target site and in effect, the availability of the drug to the tissues or organs of the body cannot be prolonged and predicted over a period of time [1].

In controlled and sustained drug delivery, drugs are mostly contained in vehicles or carriers that together are administered to the patient either by injection or implantation. The carriers form a drug vehicle that encapsulates the drug and keeps it sheltered from outside influences. The drug is then released into the vehicle and makes it available to the body at a controlled rate. The essence of controlled and sustained release is to be able to delay the rate at which drug is being released from the vehicle by controlling certain factors contained in the delivery package [3, 4, 5].

Natural, commercial, synthetic, and clay-polymer composites/nanocomposites, films and hydrogel composites are used as formulations that prolong the release of drugs and their availability. Examples of some of these minerals include; montmorillonite (MMT) [6, 7], zeolite [8, 9, 10], bentonite [11], halloysite nanotube (HNT) [12, 13, 14] etc. Numerous studies have shown that these clays are cytocompatible and biocompatible.

Among all these minerals, halloysite nanotube (HNT) is a cost effective and biocompatible natural mineral for sustained release of active agents. HNTs offers unique properties including biocompatibility, high surface area and ability to interact with molecules of drug, either by surface adsorption or ion exchange reaction [15]. Halloysite, formed naturally in the earth over millions of years, are novel and multipurpose nanomaterials that are made up of double layer of aluminum, silicon, hydrogen and oxygen. They are ultra-tiny hollow tubes with diameters smaller than 100 nanometers (100 billionths of a meter) [16, 17].

The stoichiometry of halloysite is $\text{Al}_2\text{Si}_2\text{O}_5(\text{OH})_4 \cdot n\text{H}_2\text{O}$ and occurs in two forms: the anhydrous form with an interlayer spacing of $\sim 7 \text{ \AA}$ and the hydrated form with an enlarged interlayer spacing of 10 \AA , due to the integration of water in the inter-lamellar spaces [18].

Some other advantages are their fine particle size, high surface area, high surface to volume ratio and a wonderful dispersion rate. They maintain uniform, sustained release rate and no initial overdose, and are capable of protecting active agents within its lumen during harsh materials processing conditions. As an example, to reduce aqueous solubility and miscibility of dispersants, the lumen of halloysite nanotubes has been loaded with dispersant and their application in oil spill remediation examined [19, 20, 21, 22, 23]. Halloysite nanotubes are also capable of loading multiple active agents simultaneously and also have superb loading rates, fast adsorption rate and high adsorption capacity as compared to other nano-carriers [24]. In each layer of halloysite nanotube, the SiOH groups are found on the external surface while the AlOH groups are located on the internal surfaces. Because of this, the chemistry of the inner lumen and that of the outer surfaces are completely different. The inner surface is positively charged, and the outer surface is negatively charged. The positive charge of the inner lumen is a result of protonation of the Al-OH groups at low pH. When the pH increases above 2, deprotonation of the Si-OH groups occurs on the outer surface, making it negatively charged. The properties of the inner and outer surface of halloysite nanotubes can be altered by exploiting electrostatic and covalent interactions between the surfaces of HNT and other molecules. This can result in the creation of hydrophobic and hydrophilic surfaces [25]. Properties of halloysite nanotubes can further be enhanced by forming composite with polymers like poly lactic-co-glycolic acid (PLGA), polyvinyl alcohol, epoxy, polyamides, polyacrylates and biopolymers such as chitosans, polysaccharides etc. [12, 26, 27, 28, 29, 30, 31]. Forming composites of halloysite nanotubes with other polymers enhances active agents' interaction with halloysite leading to an extended release of these loaded active agents from their lumen. Surface modifying these halloysite nanotubes improves their properties for loading and sustain release application. There are different techniques for modifying the surface of halloysite nanotubes for different applications. These surface modification techniques include: protonation and deprotonation, acid-treatment, forming composite with other materials, etc. Any of these techniques gives halloysite a special advantage that can be exploited in the controlled and sustained release application of active agents. Although these surface modification techniques are believed to improve sustain release of active agents, comparison of the effectiveness of any of these techniques over the others has not been well established [12]. In this study therefore, we modified the HNT surface using acid-treatment and polymer/HNT composite formation techniques. We evaluated the loading efficiency of raw untreated HNT, acid treated HNT and HNT/polymer composite and finally evaluate the release characteristics

of drug loaded HNT, drug loaded acid-treated HNT, and drug loaded HNT/polymer composites

2. Materials and methods

2.1. Materials

Halloysite nanotube ($\text{Al}_2\text{Si}_2\text{O}_5(\text{OH})_4 \cdot 2\text{H}_2\text{O}$) with 99.5% purity, sodium salicylate drug ($\text{C}_7\text{H}_5\text{NaO}_3$) with 99.5% purity, and polyvinyl alcohol (polymer) were obtained from Sigma Aldrich, MO, U.S.A. Sulfuric acid (H_2SO_4) with 98% purity and ethanol ($\text{C}_2\text{H}_6\text{O}$) 95% purity were obtained from VWR, U.S.A.

2.2. Loading of sodium salicylate onto unmodified halloysite nanotube

Approximately 1 g of the sodium salicylate drug was dissolved in 50 ml of 4:1 v/v ethanol - water mixture to form 20 mg/ml saturated drug solution. Approximately 2.5 ml of the saturated drug solution was added to 1 g of dry powdered halloysite nanotubes. A beaker containing the suspension of halloysite and saturated sodium salicylate drug solution was transferred into vacuum desiccator. Several cycles of vacuum suction and release was applied in several intervals until there was no fizzing. The resulting material was then thoroughly mixed and left to dry under vacuum at 37 °C. The HNT-drug loaded material was ground using mortar and pestle. The procedure was repeated using 2.5 ml aliquot of the drug solution.

2.3. Acid treatment of halloysite nanotubes

1 g of halloysite nanotubes were dispersed in 0.01 M sulfuric acid. The as-formed suspension was magnetically stirred on hot plate at 40 °C for about one hour. The acid-treated halloysite was washed several times with deionized water until the pH of the supernatant was close to neutral (that is pH of ~ 7). The sample was then dried in an oven at 50 °C for 24 hrs. This treated halloysite was named Acid-Treated HNT. The sodium salicylate drug was then loaded onto the acid-treated halloysite using the procedure already described above (section 2.2).

2.4. Preparation of drug halloysite polymer composite

Solution casting was used to prepare the drug loaded halloysite (DLH)/polyvinyl alcohol (PVA) polymer composite. Typically, a stock solution of PVA was prepared by dissolving 1 g of the PVA in 10 ml deionized water at 85 °C. The formed solution was cooled to room temperature. The drug loaded halloysite (DLH) was added to the polymer solution and mixed thoroughly to obtain a uniform mixture. The solution is

then cast in a polycarbonate petri dish and dried at 40 °C until the weight of the formed composite became constant.

2.5. Drug release studies

Approximately 150 mg of DLH was added to 200 ml of phosphate buffer at a physiological pH of 7.4. The mixture was magnetically stirred at 50 rpm. A sample of the stirred DLH-phosphate buffer was fetched at different time intervals and centrifuged at 5000 rpm for about 2 minutes. After centrifugation, 500 μ l of the supernatant was fetched and added to 10 ml of 1 M FeCl₃ solution. The concentration of the sodium salicylate drug was measured using UV–vis, at an absorbance wavelength of 535 nm. The same volume of DLH fetched was replaced before subsequent analysis. The above procedure was repeated but using drug loaded acid treated HNT and drug loaded HNT-polymer composite. The release studies were conducted in duplicate. The raw halloysite nanotubes, drug loaded halloysite nanotubes and the drug loaded modified halloysite nanotubes were characterized with SEM, TEM and FTIR.

Please contact the corresponding author at "enyankson@ug.edu.gh" for more information on the data used in this study.

3. Results and discussion

3.1. Structural and morphological characterization before drug loading

The powdered halloysite nanotube and sodium salicylate drug as obtained were characterized before and after the modification. Fig. 1 shows the micrographs acquired from SEM (a), TEM (b) and EDS (c) analyses of the raw untreated halloysite nanotube before loading.

The SEM and TEM micrographs above show that halloysite nanotube has a tubular cylindrical structure with open ends. The length of halloysite nanotube ranges from 500 nm to 1200 nm with an inner diameter ranging from 15 nm to 35 nm. It has a wall of thickness, 10–15 nm. These are similar to values reported in the literature [24, 32]. It should however be noted that, the size of halloysite nanotubes reported in this study is specific to our source of HNT (Sigma Aldrich) and may differ from HNTs obtained from other sources. Sigma Aldrich HNT obtained from Applied Minerals has a wide distribution in HNT length and hence may affect result reproducibility during clinical application. EDS results also shows that halloysite nanotube is predominantly composed of silicon (~33 wt.%) and aluminum (~29 wt.%).

Fig. 2 below also shows SEM micrograph of sodium salicylate drug. From the SEM, the drug has flaky morphology. This micrograph indicates the presence of sodium (22.08 wt.%) and oxygen (14.69 wt.%).

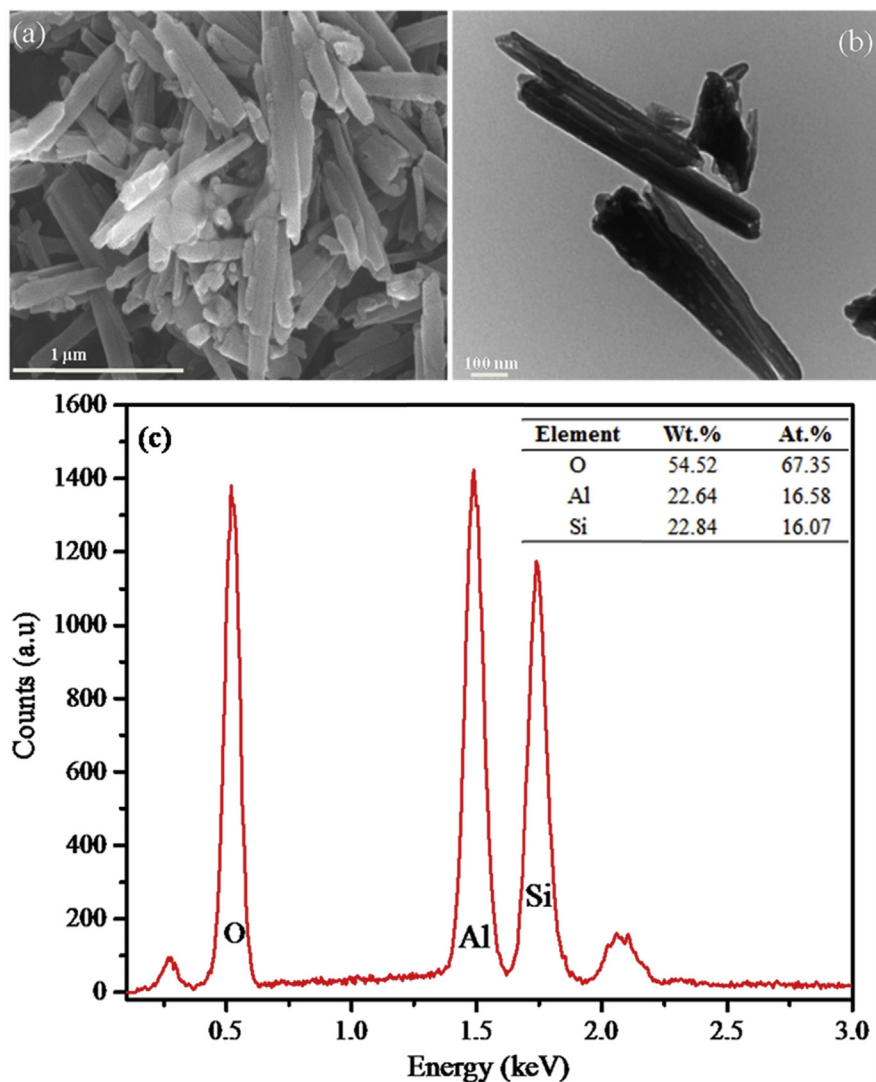


Fig. 1. (a) SEM micrograph, (b) TEM micrograph, and (c) EDS results of raw untreated halloysite nanotube.

3.2. Structural and morphological characterization of HNTs after drug loading

Sodium salicylate drug was loaded into the lumen of the raw untreated halloysite nanotube. The drug loaded halloysite nanotubes were analyzed with SEM, TEM and EDS and the results presented in Fig. 3. It is shown from the EDS results in Fig. 3 (c) that, after loading sodium salicylate drug into raw untreated halloysite nanotube, silicon, aluminum and sodium were the dominant constituents of the drug-loaded halloysite. Fig. 3 (c) shows that 7.57% by weight was the percentage of drug loaded into the halloysite nanotube. SEM and TEM micrograph also shows that, loading drugs into halloysite nanotubes does not change the morphology of

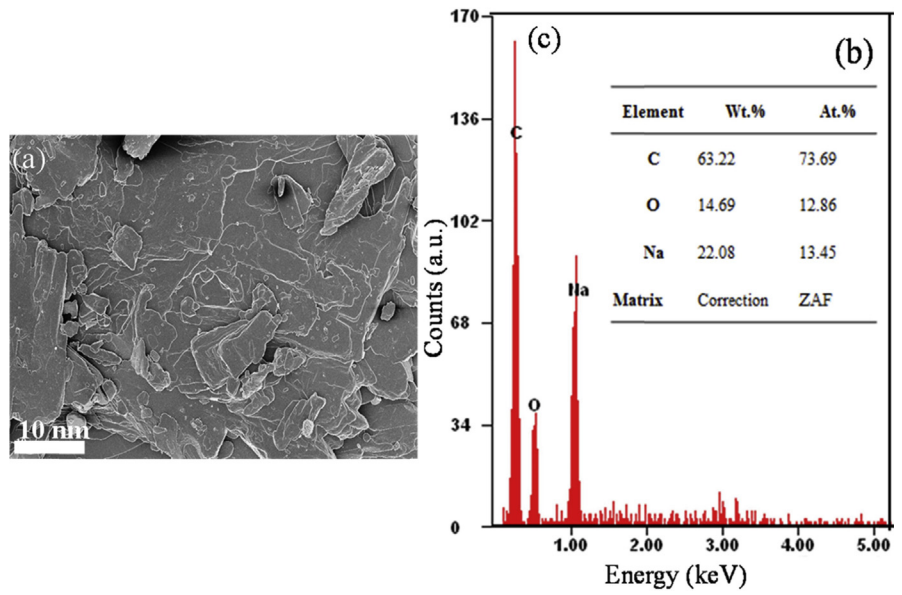


Fig. 2. (a) SEM micrograph, (b) and (c) EDS results of sodium salicylate.

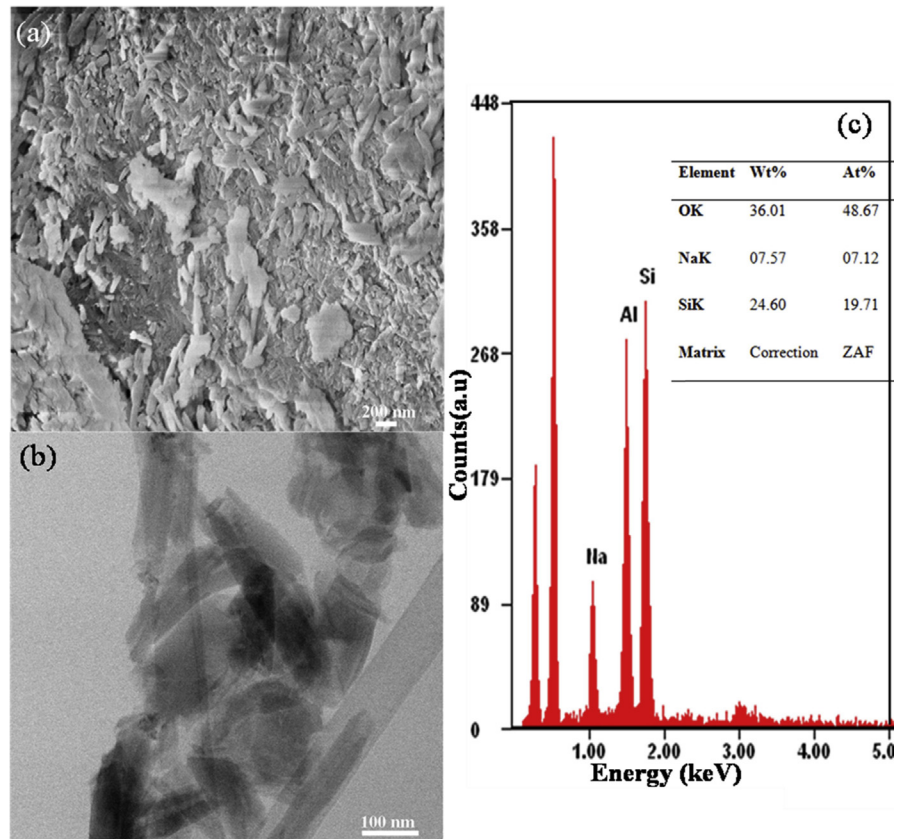


Fig. 3. (a) SEM micrograph, (b) TEM micrograph, (c) EDS results of drug loaded halloysite.

halloysite nanotube. Most importantly, its cylindrical tubular structure was maintained. TEM results in 3.0 (a) show the halloysite morphology was maintained with dispersion of drug within and around it (darker portion of the TEM image). From the drug loading technique adopted [33], the drug was loaded primarily into the lumen, interstitial spaces and the outer surface of halloysite as can be seen in Fig. 3. The drug loaded on the outside of the HNT resulted in the agglomeration of the drug loaded HNT. The agglomeration of the drug-loaded HNT is expected to influence the drug release rate since drugs located in the “inner part” of the agglomerated drug loaded HNT will have a relatively longer diffusion path and hence reduce the drug release rate.

Halloysite nanotubes were then acid-treated and loaded with sodium salicylate drug. Fig. 4 shows (a) SEM, (b) TEM, (c) EDS results of the drug loaded acid-treated

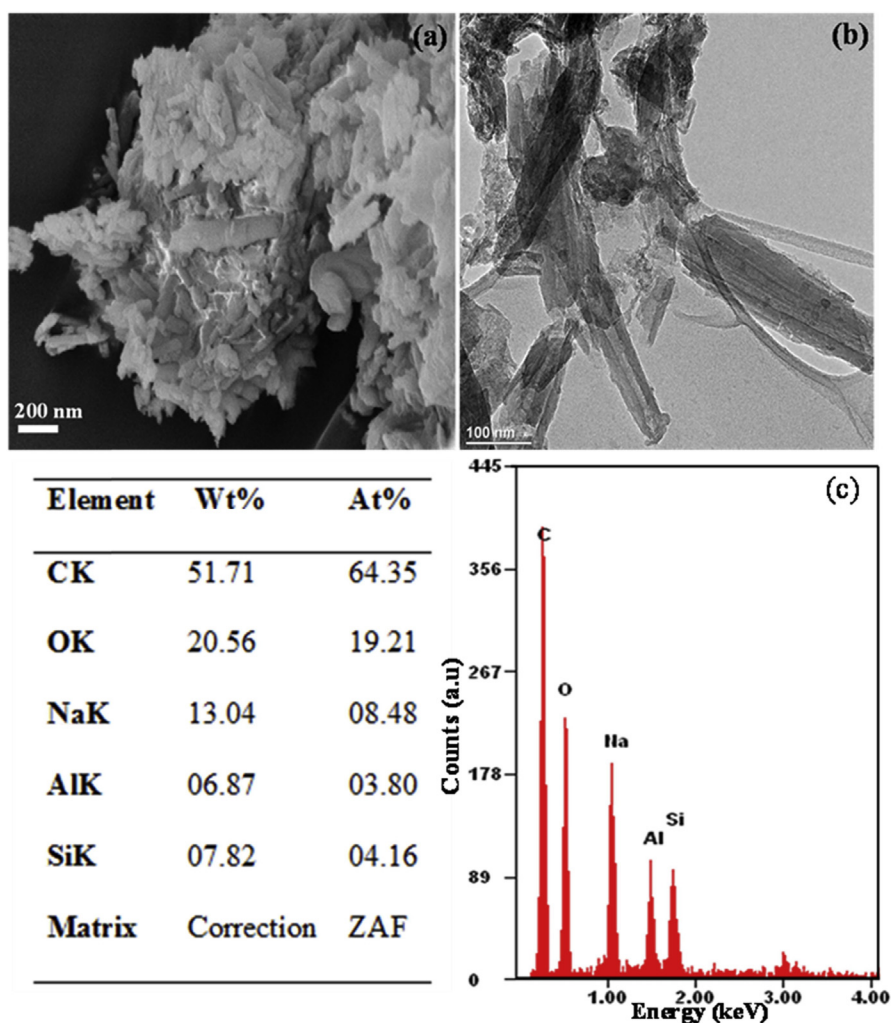


Fig. 4. (a) SEM micrograph, (b) TEM micrograph, (c) EDS results of drug loaded acid-treated halloysite.

halloysite. From the TEM results, it is seen that, the inner lumen has been enlarged. This enlargement is due to sulfuric acid reacting with the inner alumina of the halloysite. Hydrogen ions from the sulfuric acid diffuses into the halloysite pores and react with the inner alumina of the halloysite. The formed product is then washed away, and this results in the enlargement of the lumen.

The reaction occurring in the lumen is described by Eq. (1) below:



The enlarged lumen with loaded drug is evident in the TEM micrograph.

TEM results in Fig. 4 show the enlarged lumen with drug deposited in and around the halloysite nanotubes. The enlarged lumen after acid treatment is in line with already published results by Abdullayev et al. (2012) [34]. When EDS analysis was performed, it was shown that the loaded drug was 13.04 % by weight of the prepared sample. SEM results show that the structure and morphology of halloysite nanotube was maintained even after acid treatment. The dominant compositions (sodium salicylate, silicon and aluminum) of the drug loaded acid-treated halloysite nanotube were all present with their weight percentages in Fig. 4 (c).

Halloysite nanotube polymer composite was formed using solution casting. With this modification, it was hypothesized that, the polymer present in the composite forms a consistent layer around the drug-loaded halloysite. This is expected to slow down drug diffusion from the formed composite and thus, extend the drug release. Fig. 5 shows (a) SEM micrograph, (b, c) EDS results of polymer drug-loaded halloysite nanotube composite.

From the SEM micrograph in Fig. 5 (a), it is shown that the morphology is slightly changed into short cylindrical tubules with all the dominant constituents present. EDS analysis also shows that, 5.42% by weight of the prepared halloysite/Polymer composites is sodium salicylate drug.

Interaction of sodium salicylate with raw untreated halloysite and acid-treated halloysite during drug loading was further analyzed by FTIR. Pharmaceutical compounds that possess carboxylic and phenolic groups such as sodium salicylate mostly form strong complexes when they react in the presence of hydroxide minerals [35, 36]. Where halloysite shows no signal, sodium salicylate absorbs in that region of spectra. Due to this, sodium salicylate loaded unto halloysite is recognizable as shown in Fig. 6 below. The FTIR spectra of raw untreated halloysite, acid-treated halloysite and drug loaded halloysite illustrate vibrational frequencies shift with sodium salicylate and some new peaks emanating. With raw untreated halloysite, absorption spectrum at 3640 cm^{-1} and 908 cm^{-1} indicates $-\text{OH}$ group and the bending vibrations of Al-OH , respectively. Absorption spectrum at 1070 cm^{-1} and 551 cm^{-1} also indicates the Si-O stretching vibrations and Si-O bending

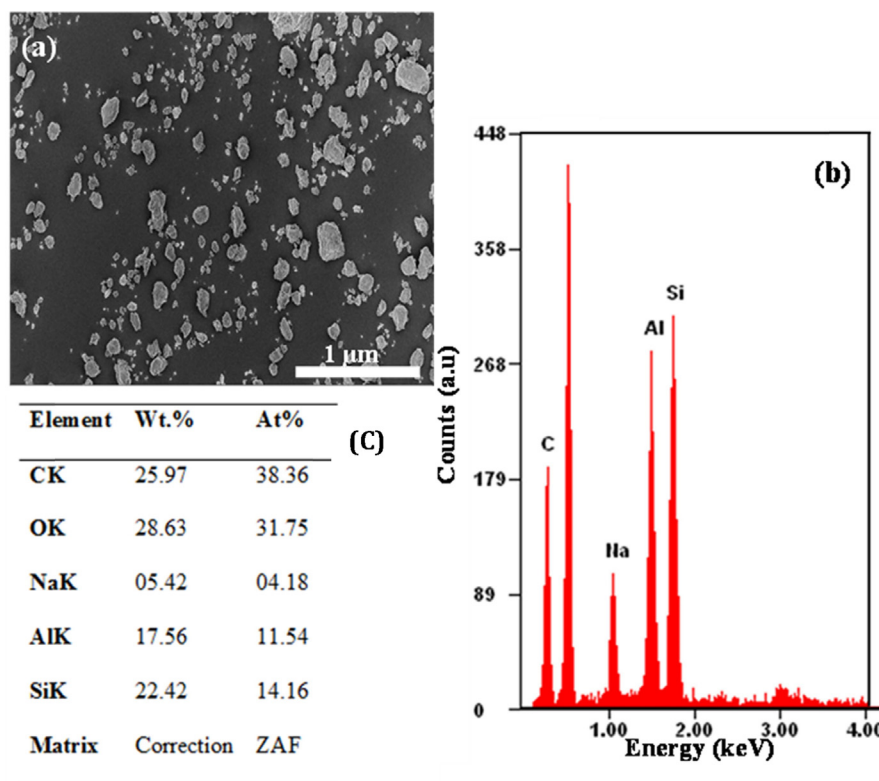


Fig. 5. (a) SEM micrograph, (b, c) EDS results of drug loaded acid-treated halloysite.

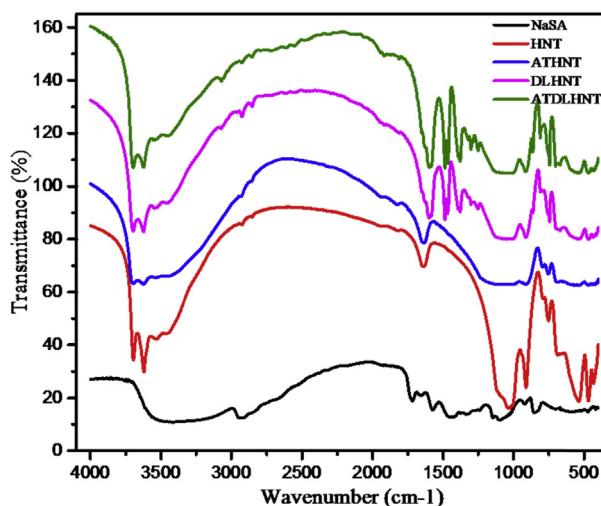


Fig. 6. FTIR spectra of raw untreated halloysite, acid-treated halloysite, drug loaded halloysite, acid treated drug loaded halloysite and sodium salicylate drug.

vibrations, respectively. After acid treatment of the halloysite nanotubes, the $-OH$ group and Si-O stretching vibrations had the same peaks as that of the raw untreated halloysite. The bending vibrations of Al-OH slightly shifted from 908 cm^{-1} to 883 cm^{-1} . Si-O bending vibration also shifted from 551 cm^{-1} to 575 cm^{-1} . After

loading sodium salicylate drug unto raw untreated halloysite and acid treated halloysite, there was an emanation of new peaks like Ph-OH at 1370 cm^{-1} indicating the bending mode and Ph-O at 1253 cm^{-1} from the phenolic group of sodium salicylate. This obtained result shows that the Ph-OH group takes part in the interaction between sodium salicylate and aluminum within the halloysite. This weakens the hydrogen bond during the interaction with halloysite and changes the π -electron density of the benzene ring. The absorption band of C-C vibrations (1460 cm^{-1} , 1570 cm^{-1} and 1458 cm^{-1}) were also adjusted. Fig. 6 below shows the vibrational peaks discussed above for raw untreated halloysite nanotube (HNT), acid treated halloysite nanotube (ATHNT), drug loaded halloysite nanotube (DLHNT) and acid treated drug loaded halloysite nanotube (ATDLHNT). Table 1 below also summarizes the recognizable peaks that indicate raw untreated halloysite nanotube (HNT), acid treated halloysite nanotube (ATHNT), drug loaded halloysite nanotube (DLHNT), acid treated drug loaded halloysite nanotube (ATDLHNT) and sodium salicylate drug (NaSA).

3.3. Drug loading efficiency and drug loading percentage

Drug loading efficiency and loading percentage of halloysite and its composite were calculated from Eqs. (2) and (3), respectively. These equations were obtained from a simple method provided by Shi et al. [37].

$$\text{Loading Efficiency (\%)} = \frac{M_t}{M_0} \times 100\%, \quad (2)$$

M_t and M_0 stand for the mass of encapsulated sodium salicylate drug and the total sodium salicylate drug used for encapsulation respectively.

$$\text{Loading Percentage (\%)} = \frac{M_t}{M} \times 100\%, \quad (3)$$

Table 1. Vibrational peak for raw untreated halloysite nanotubes (HNT), acid treated halloysite nanotube (ATHNT), drug loaded halloysite nanotube (DLHNT), acid treated drug loaded halloysite nanotube (ATDLHNT) and sodium salicylate drug (NaSA).

Sample	-OH group	Al-OH bending vibration	Si-O stretching vibration	Si-O bending vibration	ν Ph-OH	δ Ph-OH	ν_s -COO ⁻	ν C-C ring
HNT	3640	908	1070	551	-	-	-	-
ATHNT	3640	883	1070	575	-	-	-	-
DLHNT	3640	908	1070	551	1244	1321	1387	1650
ATDLHNT	3640	883	1070	575	1244	1321	1387	1650
NaSA	-	-	-	-	1253	1343	1387	1650

M_i and M stand for the mass of encapsulated sodium salicylate drug and total drug plus the encapsulation vehicle, respectively. M_i was calculated from Eq. (4):

$$M_i = (\text{EDS value (\%)}) \times M \quad (4)$$

Table 2 below summarizes the loading efficiency and loading percentage as described by the formulae above.

After three cycles of drug loading, it is evident in Table 2 that, the loading efficiency and loading percentage of drug loaded acid treated halloysite nanotube is higher as compared to polymer/drug loaded halloysite composite and raw untreated drug loaded halloysite.

3.4. Release characteristics of sodium salicylate drug

The release profile of sodium salicylate drug from raw untreated halloysite in comparison to acid-treated halloysite and polymer/halloysite composite are shown in Fig. 7 below. From the release profile in Fig. 7, drug release from polymer/drug-loaded halloysite is observed to be slower and longer as compared with drug-loaded halloysite and acid treated halloysite. As at 7 hours, out of 54.2 mg of drug loaded, 51.4 mg of drug was released from polymer/halloysite composite. With acid-treated halloysite, out of 130.4 mg of drug loaded, 75.7 mg was released after 5 hours. With unmodified halloysite, out of 75.7 mg of drug loaded, 70.3 mg was released after 5 hours. The release of drug from raw unmodified halloysite reached a plateau after 3 hours. With acid-treated halloysite, it reached its plateau after 4.5 hours. Rapid release is observed in drug loaded acid-treated halloysite because of an enlarged lumen, which allowed for maximum loading of drug. With polymer/drug-loaded halloysite, the release was gradual and was still increasing even after 7 hours. The slower and longer release of drug from polymer/drug-loaded halloysite may be due to the presence of the polymer, which was hypothesized to form a consistent layer around the drug loaded halloysite during the formation of the composite. Shi et al similarly report this observation [36]. According to their report, the presence of PLGA, a polymeric nanofiber in the formation of

Table 2. Entrapment efficiency and loading percentage of sodium salicylate drug.

Sample	M_i	M_o	M	Loading/Entrapment Efficiency (%)	Loading Percentage/capacity (%)
Drug Loaded Halloysite (DLHNT)	75.7	150	~ 1000	50.47	7.57
Drug Loaded Acid-Treated Halloysite (ATDLHNT)	130.4	150	~ 1000	86.93	8.69
Polymer/Drug Loaded Composite (P/DLHNT)	54.2	150	~ 1200	36.13	5.42

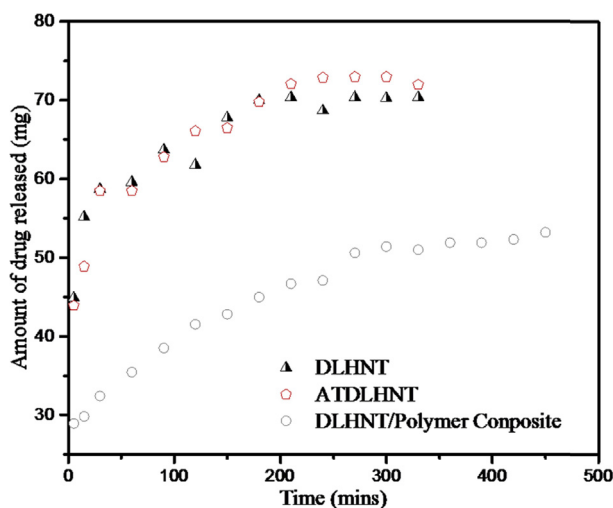


Fig. 7. Release profiles of the drugs from halloysite nanotubes, acid-treated halloysite nanotubes and polymer/halloysite nanotubes.

composite for drug release hinders the release and diffusion of drug from polymeric/halloysite composite. The same observation was made by Veerabadran et al [38]. But according to them, the polymer present in the composite formation also penetrates into the lumen of the halloysite. In the release profiles of raw untreated drug loaded halloysite and acid treated halloysite, there was an initial burst for the first 10 minutes followed by a sustained release. The initial burst implies that, some of the drug molecules are bound to the external surface of halloysite. This has already been reported by Jing et al. [39]. They reported that mostly; drug release is preceded by an initial burst release. The reported release rates in this article are similar but relatively higher than the release rates reported by Makaremi et al [40], who loaded salicylic acid into thin and long halloysite nanotubes and then formed a biofilm using apple pectin. The differences in the release rate of salicylic acid may be due to the differences in the dimensions of the halloysite nanotubes used and the fact that we used polyvinyl alcohol in forming the composite while they used pectin. In addition, the method used in conducting their release studies was entirely different from the one used in our study. Dзамukova et al [41] loaded brilliant green into halloysite nanotubes and end capped the halloysite nanotubes with dextrin. Approximately 30 % of the loaded brilliant green was released in 24 hours. This release rate was significantly slower than the ones reported in this study (for salicylate acid loaded into HNT-polymer composite). A related study has been reported by Cavallaro et al [42]. In their study, halloysite nanotube was loaded with $\text{Ca}(\text{OH})_2$ and end capped with calcium triphosphate salt. End capping extended the release of $\text{Ca}(\text{OH})_2$ with 10 % $\text{Ca}(\text{OH})_2$ released in 60 min and this helped in deacidification of paper.

The release profile of polymer/drug loaded halloysite is slightly linear which means the release remains constant over time. This is a good behavior for sustained drug

release. The amount of sodium salicylate released during the release studies is in the order, acid-treated halloysite > raw untreated halloysite > polymer/halloysite composite. This result means that acid treated halloysite has a higher amount of drug released than raw halloysite and polymer/halloysite composite, but the release was not sustained for a longer period of time as that of polymer/halloysite composite. Polymer coating thickness will also affect the drug release with larger polymer coating thickness (longer drug diffusion path) expected to sustain the drug release much longer than a relatively smaller coating thickness (shorter drug diffusion path). However, we did not estimate the polymer coating thickness and hence can't provide detailed discussion on the effect of polymer thickness in this study.

3.5. Kinetic model for drug release profiles

In vitro release results that were obtained from drug release studies were fitted into kinetic models such as Zero-Order, First-Order, Higuchi equation and Koresmeyer-Peppas equation. Regression analysis was used to obtain correlation coefficients.

For each of the plots, Q_t is the amount of sodium salicylate drug released at time t . Figs. 8, 9, 10, and 11 below are plots for the models: zero order, first order, Higuchi and Koresmeyer-Peppas, respectively, Table 3 summarizes the rate constants obtained from plots of Figs. 8, 9, 10, and 11.

From the different kinetic models plots in Figs. 8, 9, 10, and 11 and Table 3, correlation coefficients of acid-treated drug loaded halloysite showed higher correlation with Higuchi model ($R^2 = 0.9653$) and Koresmeyer-Peppas model ($R^2 = 0.9682$) plots than zero-order ($R^2 = 0.7790$) and first-order ($R^2 = 0.9252$). On the other hand, polymer/drug-loaded composite showed higher correlation with Higuchi model ($R^2 = 0.9947$), first-order ($R^2 = 0.9949$) and Koresmeyer-Peppas ($R^2 = 0.9933$) than zero-order model ($R^2 = 0.8997$). This showed that the release

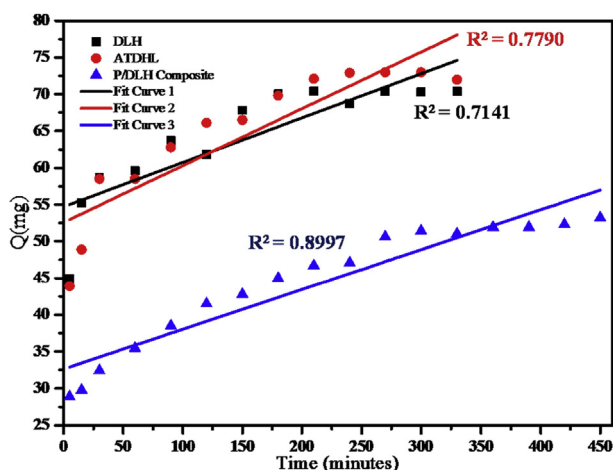


Fig. 8. Zero order model for DLHNT, ATDLHNT, P/DLHNT composite.

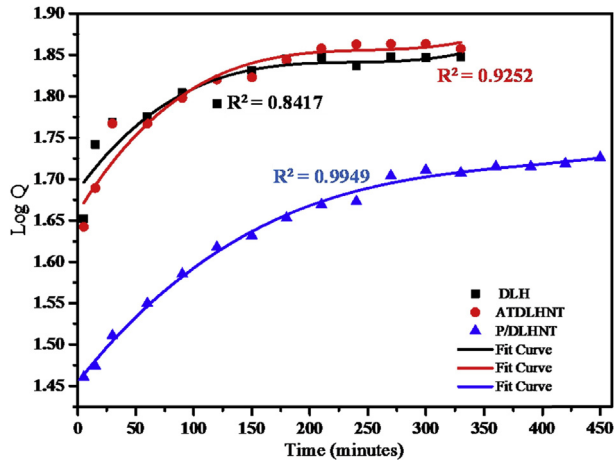


Fig. 9. First order model for DLHNT, ATDLHNT, P/DLHNT composite.

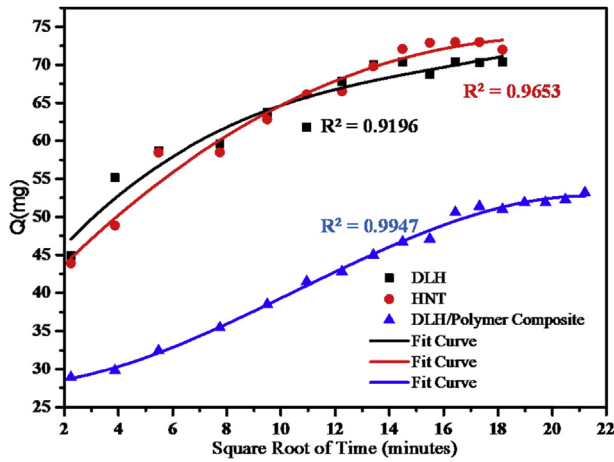


Fig. 10. Higuchi model for DLHNT, ATDLHNT, P/DLHNT composite.

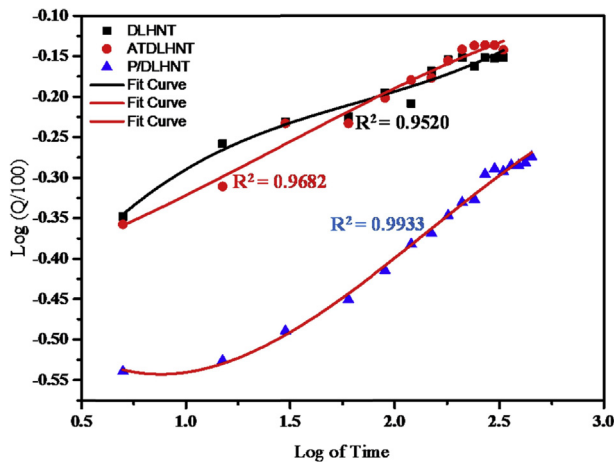


Fig. 11. Korsmeyer-Peppas model for DLHNT, ATDLHNT, P/DLHNT composite.

Table 3. Rate constants of different kinetic models.

Sample	Zero Order	First-Order	Higuchi Equation	Korsemyer-Peppas Equation
	K_0	K_1	K_H	K_p
DLHNT	0.060 ± 0.005	0.06 ± 0.013	40.09 ± 2.69	0.153 ± 0.018
ATDLHNT	0.077 ± 0.019	0.083 ± 0.017	35.92 ± 1.27	0.864 ± 0.124
P/DLHNT	0.054 ± 0.014	0.058 ± 0.022	20.34 ± 2.02	0.234 ± 0.095

[DLHNT-Drug Loaded Halloysite Nanotube] [ATDLHNT-Acid Treated Drug Loaded Halloysite Nanotube] [P/DLHNT-Polymer/Drug Loaded HNT Composite].

mechanism for acid treated drug loaded halloysite and polymer/drug loaded halloysite obey the Fickian diffusion model since they show higher correlation for Higuchi and Korsemyer-Peppas models.

With drug-loaded halloysite, correlation coefficient showed higher correlation with Korsemyer-Peppas ($R^2 = 0.9520$) than zero-order ($R^2 = 0.7141$), first-order ($R^2 = 0.8417$) and Higuchi ($R^2 = 0.9196$). This showed that the release mechanism of drug loaded halloysite is also Fickian diffusion with exponent $n = 0.46$ for such plots. It is very clear from the correlations (R^2) presented in Table 3 above that the drug release rate from DLHNT, ATDLHNT and P/DLHNT do not obey the zero-order mode. A zero order release kinetics refers to the process of constant drug release from a drug release device [43]. It is obvious from the release profiles presented in Fig. 7 that the drug release rate from halloysite nanotubes, acid treated halloysite nanotubes and polymer/halloysite nanotubes composite were not constant. The release profile observed in Fig. 7 is best described by the Higuchi and Korsemyer-Peppas models which are diffusion controlled [44]. The Higuchi model describes the rate of release of drug from a matrix where the drug loading exceeds its solubility in the matrix into a surrounding fluid [45, 46]. The halloysite and polymer composite is the matrix in this study. The rate of release of the drug into the surrounding fluid is governed by the Fick's law of diffusion. As already stated, the drug release from the materials studied show Fickian diffusion. Fickian diffusion means that, drug loaded into the drug delivery vehicle is released by diffusion transport in a gradual and steady manner. That is the drug diffuses out of the halloysite nanotubes and the halloysite nanotube/polymer composite. This explains the initial burst and the gradual release observed at the initial and later stages of the release, respectively. This observation can be attributed to the large concentration difference as depicted by the Fick's Laws of diffusion in the initial stages of the release. As the concentration gradient decreases as more drug is released into the surrounding media, the diffusion rate decreases and this affects the release rate. By comparison, the rate constant values reported in this study is significantly lower than those reported in a study conducted by Cavallaro et al [47]. They investigated the release kinetics of doxycycline loaded into Calcium Alginate confined within HNTs.

4. Conclusion

In conclusion, two surface modification techniques were used to improve the sustain release properties of halloysite nanotube. These modification techniques were acid treatment technique and polymer/halloysite Composite formation. SEM and TEM micrographs from these modifications showed that, acid treatment enlarged the lumen of halloysite. This improved the drug loading and thus the subsequent large amount released. This makes acid treated halloysite a suitable vehicle for sustain-release of large amount of drugs and other active agents. With polymer/halloysite composite, the polymer used formed a consistent layer around the halloysite and this delayed the release of drug and hence an extended release of drug was observed. The sustain release of drugs from the formed composite was longer than acid treated halloysite, but the amount of drug released from acid treated halloysite was more than polymer/halloysite composite. In all these modifications, the morphology of halloysite was maintained for the different characterizations used in the analysis. Finally, modified halloysite offers a sustained release of drugs either by increasing the amount of drugs released in a sustained manner or extending the sustain release of these drugs and the release was diffusion controlled.

Declarations

Author contribution statement

Ernest Gyan Bediako: Performed the experiments; Analyzed and interpreted the data; Wrote the paper.

Emmanuel Nyankson: Conceived and designed the experiments; Performed the experiments; Analyzed and interpreted the data; Contributed reagents, materials, analysis tools or data; Wrote the paper.

David Dodoo-Arhin: Conceived and designed the experiments; Performed the experiments; Analyzed and interpreted the data; Wrote the paper.

Dariusz Łukowiec, Błażej Tomiczek: Contributed reagents, materials, analysis tools or data.

Benjamin Agyei-Tuffour: Conceived and designed the experiments; Analyzed and interpreted the data; Wrote the paper.

Abu Yaya: Conceived and designed the experiments; Analyzed and interpreted the data.

Johnson K. Efavi: Analyzed and interpreted the data.

Funding statement

This research did not receive any specific grant from funding agencies in the public, commercial, or not-for-profit sectors.

Competing interest statement

The authors declare no conflict of interest.

Additional information

No additional information is available for this paper.

References

- [1] A. Deshpande, et al., Controlled-release drug delivery systems for prolonged gastric residence: an overview, *Drug Dev. Ind. Pharm.* 22 (6) (1996) 531–539.
- [2] X. Huang, C.S. Brazel, On the importance and mechanisms of burst release in matrix-controlled drug delivery systems, *J. Contr. Release* 73 (2) (2001) 121–136.
- [3] G. Tiwari, et al., Drug delivery systems: an updated review, *Int. J. Pharm. Investig.* 2 (1) (2012) 2–11.
- [4] S. Fredenberg, et al., The mechanisms of drug release in poly (lactic-co-glycolic acid)-based drug delivery systems—a review, *Int. J. Pharm.* 415 (1) (2011) 34–52.
- [5] J. Patil, et al., Ionotropic gelation and polyelectrolyte complexation: the novel techniques to design hydrogel particulate sustained, modulated drug delivery system: a review, *Digest J. Nanomater. Biostructures* 5 (1) (2010) 241–248.
- [6] R.I. Iliescu, et al., Montmorillonite–alginate nanocomposite as a drug delivery system—incorporation and in vitro release of irinotecan, *Int. J. Pharm.* 463 (2) (2014) 184–192.
- [7] S. Hua, et al., Controlled release of ofloxacin from chitosan–montmorillonite hydrogel, *Appl. Clay Sci.* 50 (1) (2010) 112–117.
- [8] C.-Y. Sun, et al., Zeolitic imidazolate framework-8 as efficient pH-sensitive drug delivery vehicle, *Dalton Trans.* 41 (23) (2012) 6906–6909.
- [9] R. Ananthoji, et al., Symbiosis of zeolite-like metal–organic frameworks (rho-ZMOF) and hydrogels: composites for controlled drug release, *J. Mater. Chem.* 21 (26) (2011) 9587–9594.

- [10] M. Arruebo, Drug delivery from structured porous inorganic materials, Wiley Interdiscip. Rev. Nanomed. Nanobiotechnol. 4 (1) (2012) 16–30.
- [11] S.-T. Oh, et al., The preparation of polyurethane foam combined with pH-sensitive alginate/bentonite hydrogel for wound dressings, Fibers Polym. 12 (2) (2011) 159.
- [12] E. Abdullayev, Y. Lvov, Halloysite clay nanotubes as a ceramic “skeleton” for functional biopolymer composites with sustained drug release, J. Mater. Chem. B 1 (23) (2013) 2894–2903.
- [13] Y. Lvov, E. Abdullayev, Functional polymer–clay nanotube composites with sustained release of chemical agents, Prog. Polym. Sci. 38 (10) (2013) 1690–1719.
- [14] R. Yendluri, et al., Paclitaxel encapsulated in halloysite clay nanotubes for intestinal and intracellular delivery, J. Pharmaceut. Sci. 106 (10) (2017) 3131–3139.
- [15] R. Singh, J.W. Lillard, Nanoparticle-based targeted drug delivery, Exp. Mol. Pathol. 86 (3) (2009) 215–223.
- [16] M. Du, B. Guo, D. Jia, Newly emerging applications of halloysite nanotubes: a review, Polym. Int. 59 (5) (2010) 574–582.
- [17] R. Kamble, et al., Halloysite nanotubes and applications: a review, J. Adv. Sci. Res. 3 (2) (2012) 25–29.
- [18] Y.M. Lvov, et al., Halloysite clay nanotubes for controlled release of protective agents, ACS Nano 2 (5) (2008) 814–820.
- [19] O. Owoseni, et al., Release of surfactant cargo from interfacially-active halloysite clay nanotubes for oil spill remediation, Langmuir 30 (45) (2014) 13533–13541.
- [20] E. Nyankson, et al., Surfactant-loaded halloysite clay nanotube dispersants for crude oil spill remediation, Ind. Eng. Chem. Res. 54 (38) (2015) 9328–9341.
- [21] O. Owoseni, et al., Interfacial adsorption and surfactant release characteristics of magnetically functionalized halloysite nanotubes for responsive emulsions, J. Colloid Interface Sci. 463 (2016) 288–298.
- [22] E. Nyankson, D. Rodene, R.B. Gupta, Advancements in crude oil spill remediation research after the Deepwater Horizon oil spill, Water Air Soil Pollut. 227 (1) (2016) 29.
- [23] E. Nyankson, Smart Dispersant Formulations for Reduced Environmental Impact of Crude Oil Spills, 2015.

- [24] D. Rawtani, Y. Agrawal, Multifarious applications of halloysite nanotubes: a review, *Rev. Adv. Mater. Sci.* 30 (3) (2012) 282–295.
- [25] G. Lazzara, et al., An assembly of organic-inorganic composites using halloysite clay nanotubes, *Curr. Opin. Colloid Interface Sci.* 35 (2018) 42–50.
- [26] R. Qi, et al., Biocompatibility of electrospun halloysite nanotube-doped poly (lactic-co-glycolic acid) composite nanofibers, *J. Biomater. Sci. Polym. Ed.* 23 (1–4) (2012) 299–313.
- [27] R. Qi, et al., Electrospun poly (lactic-co-glycolic acid)/halloysite nanotube composite nanofibers for drug encapsulation and sustained release, *J. Mater. Chem.* 20 (47) (2010) 10622–10629.
- [28] H. Aloui, et al., Synergistic effect of halloysite and cellulose nanocrystals on the functional properties of PVA based nanocomposites, *ACS Sustain. Chem. Eng.* 4 (3) (2016) 794–800.
- [29] R. Zhai, et al., Chitosan–halloysite hybrid-nanotubes: horseradish peroxidase immobilization and applications in phenol removal, *Chem. Eng. J.* 214 (2013) 304–309.
- [30] M. Liu, et al., Chitosan–halloysite nanotubes nanocomposite scaffolds for tissue engineering, *J. Mater. Chem. B* 1 (15) (2013) 2078–2089.
- [31] M. Liu, et al., Chitosan/halloysite nanotubes bionanocomposites: structure, mechanical properties and biocompatibility, *Int. J. Biol. Macromol.* 51 (4) (2012) 566–575.
- [32] M. Du, B. Guo, D. Jia, Thermal stability and flame retardant effects of halloysite nanotubes on poly (propylene), *Eur. Polym. J.* 42 (6) (2006) 1362–1369.
- [33] C.J. Ward, S. Song, E.W. Davis, Controlled release of tetracycline–HCl from halloysite–polymer composite films, *J. Nanosci. Nanotechnol.* 10 (10) (2010) 6641–6649.
- [34] E. Abdullayev, et al., Enlargement of halloysite clay nanotube lumen by selective etching of aluminum oxide, *ACS Nano* 6 (8) (2012) 7216–7226.
- [35] G. Cavallaro, et al., Modified halloysite nanotubes: nanoarchitectures for enhancing the capture of oils from vapor and liquid phases, *ACS Appl. Mater. Interfaces* 6 (1) (2013) 606–612.
- [36] D. Philip, et al., FT-Raman, FT-IR and surface enhanced Raman scattering spectra of sodium salicylate, *Spectrochim. Acta Mol. Biomol. Spectrosc.* 57 (8) (2001) 1561–1566.

- [37] Y.-F. Shi, et al., Functionalized halloysite nanotube-based Carrier for intracellular delivery of antisense oligonucleotides, *Nanoscale Res. Lett.* 6 (1) (2011) 608.
- [38] N.G. Veerabadran, et al., Organized shells on clay nanotubes for controlled release of macromolecules, *Macromol. Rapid Commun.* 30 (2) (2009) 99–103.
- [39] H. Jing, et al., Internally modified halloysite nanotubes as inorganic nanocontainers for a flame retardant, *Chem. Lett.* 42 (2) (2013) 121–123.
- [40] M. Makaremi, et al., Effect of morphology and size of halloysite nanotubes on functional pectin bionanocomposites for food packaging applications, *ACS Appl. Mater. Interfaces* 9 (20) (2017) 17476–17488.
- [41] M.R. Dзамukova, et al., Enzyme-activated intracellular drug delivery with tubule clay nanoformulation, *Sci. Rep.* 5 (2015) 10560.
- [42] G. Cavallaro, et al., Halloysite nanotubes: controlled access and release by smart gates, *Nanomaterials* 7 (8) (2017) 199.
- [43] G. Singhvi, M. Singh, In-vitro drug release characterization models, *Int. J. Pharm. Stud. Res.* 2 (1) (2011) 77–84.
- [44] T. Hayashi, et al., Formulation study and drug release mechanism of a new theophylline sustained-release preparation, *Int. J. Pharm.* 304 (1) (2005) 91–101.
- [45] D. Paul, Elaborations on the Higuchi model for drug delivery, *Int. J. Pharm.* 418 (1) (2011) 13–17.
- [46] J.H. Petropoulos, K.G. Papadokostaki, M. Sanopoulou, Higuchi's equation and beyond: overview of the formulation and application of a generalized model of drug release from polymeric matrices, *Int. J. Pharm.* 437 (1) (2012) 178–191.
- [47] G. Cavallaro, et al., Nanohydrogel formation within the halloysite lumen for triggered and sustained release, *ACS Appl. Mater. Interfaces* 10 (9) (2018) 8265–8273.